Phosphorylated Presenilin 1 decreases β-amyloid by facilitating autophagosome–lysosome fusion

Victor Bustos[a,1], Maria V. Pulina[a], Ashley Bispo[a], Alison Lam[a], Marc Flajolet[a], Fred S. Gorelick[b,c], and Paul Greengard[a,1]

[a]Laboratory of Molecular and Cellular Neuroscience, The Rockefeller University, New York, NY 10065; [b]Department of Internal Medicine, Yale University School of Medicine, New Haven, CT 06520; and [c]Department of Cell Biology, Yale University School of Medicine, New Haven, CT 06520

Contributed by Paul Greengard, April 27, 2017 (sent for review March 30, 2017; reviewed by Yue-Ming Li and Sangram S. Sisodia)

Presenilin 1 (PS1), the catalytic subunit of the γ-secretase complex, cleaves βCTF to produce Aβ. We have shown that PS1 regulates Aβ levels by a unique bifunctional mechanism. In addition to its known role as the catalytic subunit of the γ-secretase complex, selective phosphorylation of PS1 on Ser367 decreases Aβ levels by increasing βCTF degradation through autophagy. Here, we report the molecular mechanism by which PS1 modulates βCTF degradation. We show that PS1 phosphorylated at Ser367, but not nonphosphorylated PS1, interacts with Annexin A2, which, in turn, interacts with the lysosomal *N*-ethylmaleimide–sensitive factor attachment protein receptor (SNARE) Vamp8. Annexin A2 facilitates the binding of Vamp8 to the autophagosomal SNARE Syntaxin 17 to modulate the fusion of autophagosomes with lysosomes. Thus, PS1 phosphorylated at Ser367 has an antiamyloidogenic function, promoting autophagosome–lysosome fusion and increasing βCTF degradation. Drugs designed to increase the level of PS1 phosphorylated at Ser367 should be useful in the treatment of Alzheimer's disease.

Presenilin 1 | phosphorylation | autophagy | autophagosome–lysosome fusion | Annexin A2

Autophagy is a highly conserved cellular mechanism in which aggregate-prone proteins and damaged organelles are targeted for cellular degradation in the lysosome (1). The autophagic process begins with an isolation membrane, also known as a phagophore, which expands to engulf intracellular cargo, such as protein aggregates and organelles, sequestering the cargo in a double-membraned autophagosome (2). The loaded autophagosome fuses with the lysosome, promoting the degradation of its content (3). The mechanisms regulating the fusion between the autophagosome and the lysosome are incompletely understood.

Organelle membrane fusion is achieved by soluble *N*-ethylmaleimide–sensitive factor attachment protein receptor (SNARE) complexes. Upon membrane contact, a specific SNARE complex in each organelle interacts with an opposing SNARE in another organelle to mediate membrane fusion. For example, it has been found that fusion between the late endosome and lysosome uses Syntaxin 7, Vti1b, and Syntaxin 8 on the late endosome and VAMP7 on the lysosome (4–8). In the autophagy pathway, it has been shown that VAMP7, VAMP8, and Vti1b play a role in autophagosome fusion in mammals (9–11). Syntaxin 17 (Stx17) and Vamp8 are reported to mediate autophagosome–lysosome fusion (12). In addition to providing the core machinery for membrane fusion, SNARE-interacting proteins can facilitate complex formation. For instance, SNAP29 and Atg14 stabilize Stx17–Vamp8 interaction and promote autophagosome–lysosome fusion (13–15).

Presenilins are intramembrane proteases. The Presenilin 1 (PS1) isoform is primarily responsible for Aβ generation in neurons and contains the catalytic activity of the γ-secretase complex (16–18). In addition to this catalytic role, PS1 can participate in cellular processes that are independent of its proteolytic activity, for instance: (*i*) calcium release from the endoplasmic reticulum stores as well as calcium entry through store-operated channels (19), (*ii*) mitochondrial function in cortical synaptic compartments (20), and (*iii*) modulation of homeostatic scaling of excitatory synapses in hippocampal neurons (21).

Here, we report that PS1 phosphorylated at Ser367 facilitates autophagosome–lysosome fusion. We show that PS1 phosphorylated at Ser367, but not nonphosphorylated PS1, interacts with Annexin A2, which, in turn, interacts with the lysosomal SNARE Vamp8. Finally, Annexin A2 facilitates the binding of Vamp8 to the autophagosomal SNARE Stx17 to modulate the fusion of autophagosomes with lysosomes.

Results

In the accompanying paper (22), we show that PS1 phosphorylation at Ser367 induces autophagic flux. To understand the molecular mechanism behind this effect, we examined neurons in the CA1 region of the hippocampus in PS1-S367A mice by transmission electron microscopy. We found membrane-bound structures containing electron-dense material whose number was greatly increased compared with WT (Fig. 1 *A* and *D* and Fig. S1). These vacuoles often had two adjacent well-circumscribed membrane-bound components; one was filled with amorphous electron dense material and was surrounded by a single-membrane bilayer, whereas the other had little electron dense content and a double-membrane bilayer (Fig. 1*B*). The component with electron-dense content contains cathepsin D (Fig. 1*C*). Together, the findings suggest that these structures are autolysosomes with incompletely fused membranes.

PS1 Phosphorylated at Ser367 Binds Annexin A2. Ser367 is located in the third intracellular loop of PS1, between transmembrane domains 6 and 7. In the recently resolved crystal structure of γ-secretase at 3.4 Å (23), the third intracellular loop was disordered

Significance

Autophagy is a catabolic process involving the formation of double-membrane–bound organelles called autophagosomes, which participate in the degradation of intracellular material through fusion with lysosomes. We have found a level of regulation of autophagosomal–lysosomal fusion where Presenilin 1 (PS1) phosphorylated at Ser367 specifically binds Annexin A2, which, through successive binding steps, facilitates this fusion. Lack of phosphorylation on PS1 1 Ser367 causes accumulation of partially fused autophagosomes and lysosomes in mouse brain and reduced autophagic flux. This inhibition of autophagy leads to decreased βCTF degradation and accumulation of toxic Aβ-peptide in the brain. This signaling pathway offers new potential drug targets for Alzheimer's disease.

Author contributions: V.B., M.V.P., M.F., F.S.G., and P.G. designed research; V.B., M.V.P., A.B., and A.L. performed research; V.B. and M.V.P. contributed new reagents/analytic tools; V.B., M.V.P., A.B., A.L., M.F., F.S.G., and P.G. analyzed data; and V.B., M.V.P., M.F., F.S.G., and P.G. wrote the paper.

Reviewers: Y.-M.L., Memorial Sloan–Kettering Cancer Center; and S.S.S., The University of Chicago.

The authors declare no conflict of interest.

Freely available online through the PNAS open access option.

See Commentary on page 6885.

[1]To whom correspondence may be addressed. Email: vbustos@rockefeller.edu or greengard@rockefeller.edu.

This article contains supporting information online at www.pnas.org/lookup/suppl/doi:10.1073/pnas.1705240114/-/DCSupplemental.

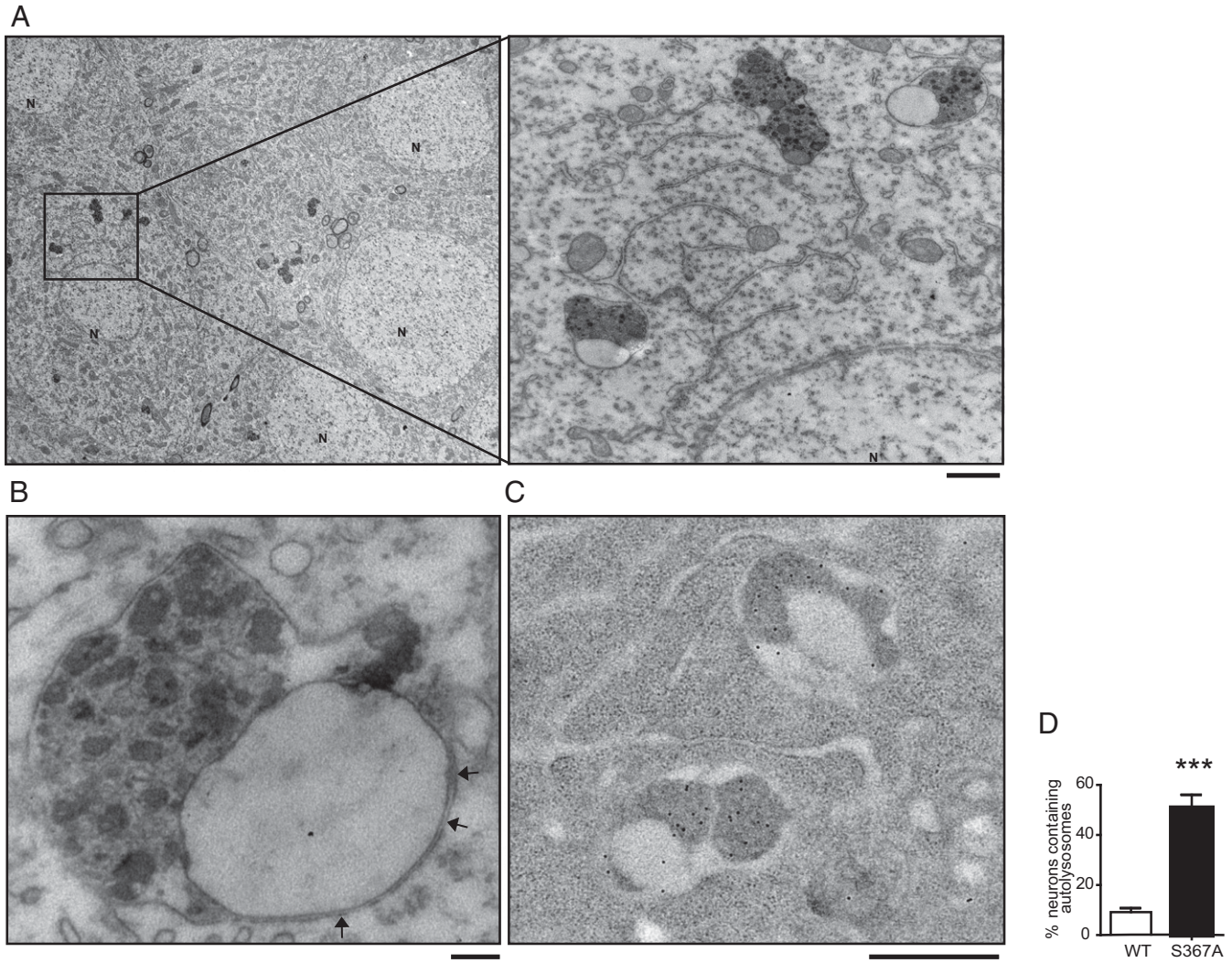

Fig. 1. Incompletely fused autophagosomes–lysosomes are increased in brains of PS1-S367A mice. (*A*) Representative electron micrographs of autolysosomes in a pyramidal neuron from the CA1 area of the hippocampus from S367A knock-in mice. (Scale bar, 500 nm.) (*B*) Higher magnification of an unfused autolysosome. Arrows point to the double membrane. (Scale bar, 100 nm.) (*C*) Autolysosomes in the CA1 area of the hippocampus in PS1-S367A mice contain Cathepsin D, as revealed by immunoelectron microscopy. (Scale bar, 500 nm.) (*D*) Quantification of the percentage of neurons bearing autolysosomes, as seen by electron microscopy. Sixty fields from three different WT and PS1-S367A mice were used for quantification. N, nucleus. Data represent mean ± SEM. ***$P < 0.001$, *t* test.

and no structure was determined. Because disordered regions can facilitate regulatory protein–protein interactions, we searched for proteins that would specifically bind to the pSer367 form of PS1.

Whole-mouse brain lysate was immunoprecipitated with an antibody recognizing the N terminus of PS1. To isolate proteins interacting with PS1 selectively in a phosphodependent manner, elution from bound PS1 was performed with a phosphopeptide containing a sequence spanning phosphorylated-Ser367 PS1. As controls, the immunoprecipitation complex was eluted with either a nonphosphorylated peptide or a scrambled peptide. Eluted proteins were separated by SDS/PAGE gel and identified by silver stain. A major 45-kDa band was eluted with the phosphorylated peptide, but not by the nonphosphorylated or scrambled peptides, and identified by mass spectrometry as Annexin A2. In addition, we generated a stable N2A cell line overexpressing the Flag-PS1 third intracellular loop, spanning amino acids 267–381 of human PS1. Lysates from these cells were used for immunoprecipitation with anti-Flag antibody. The interacting proteins were eluted with Flag peptide and subjected to SDS/PAGE and mass spectrometry analysis. Annexin A2 was again identified as an interacting protein of phosphorylated PS1. Using whole-brain lysates, we found that Annexin A2 and pPS1 coimmunoprecipitated with either anti-Annexin A2 or anti-PS1 antibodies, confirming this interaction (Fig. 2*A*).

To characterize the binding between PS1 and Annexin A2 further, we performed pull-down assays using immobilized biotinylated phosphorylated PS1 peptide on magnetic agarose beads. The beads were incubated with recombinant Annexin A2. After washing, bound proteins were separated by SDS/PAGE, levels of Annexin A2 were assessed by immunoblot, and a weak interaction was detected. Because Annexin A2 is a calcium-binding protein (24), we investigated whether calcium affected the pPS1–Annexin A2 interaction and found that 5 mM Ca^{2+} is required for maximum binding of Annexin to pPS1. No binding of Annexin A2 was detected to nonphosphorylated or scrambled peptides (Fig. 2 *B* and *C*). Mutation of PS1-S366 or PS1-S368 did not affect the binding of Annexin A2 to PS1 (Fig. 2*D*).

Annexin A2 is known to form a complex with p11, a protein that is involved in regulation of endosomal trafficking (25, 26). To determine whether p11 affects pPS1 binding to Annexin A2, we used biolayer interferometry. We found that although p11 is not necessary for Annexin A2-pPS1 binding, it does increase their binding affinity (Fig. 2*E*). To analyze the region of Annexin A2 that interacts with pPS1, we created a series of deletion constructs. Subsequent pull-down analysis indicated that the N terminus of Annexin A2 was

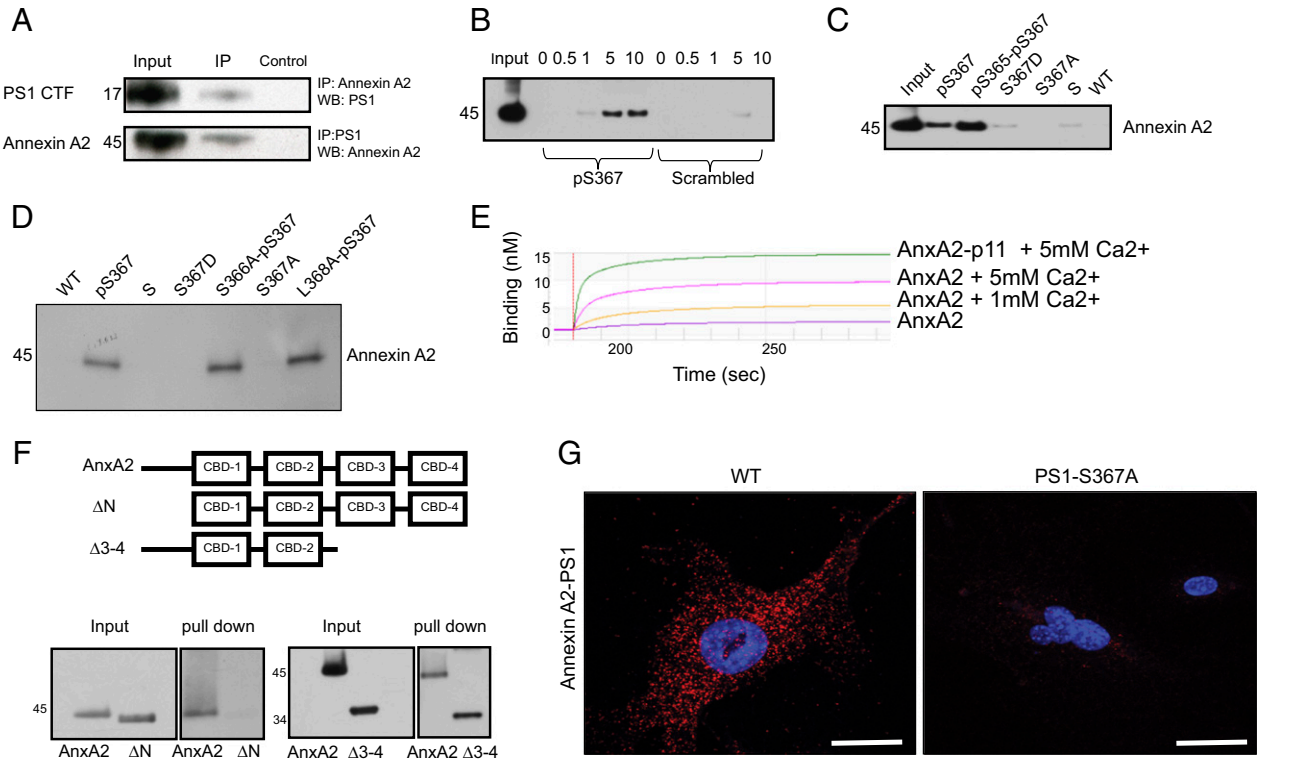

Fig. 2. PS1 phosphorylated at Ser367 binds Annexin A2. (*A*) Immunoprecipitates (IP) from whole-mouse brain lysate using anti-Annexin A2 or anti-PS1 antibody were immunoblotted with an antibody against PS1 or Annexin A2. WB, Western blot. (*B*) Pull-down, showing that increasing the concentration of calcium increases the binding between recombinant Annexin A2 and the PS1-pSer367 biotinylated peptide. Numbers indicate calcium concentration (millimolar). P, phosphorylated PS1 peptide; S, phosphorylated scrambled control peptide. (*C*) Recombinant Annexin A2 binds to both PS1-pSer367 biotinylated peptide and a double-phosphorylated PS1-pSer365-pSer367 biotinylated peptide. It does not bind to S367D or S367A biotinylated peptide or to an S or WT sequence biotinylated peptide. (*D*) Recombinant Annexin A2 binds to PS1-pSer367 biotinylated peptide and to a mutant S366A-pS367 and L368A-pS367 biotinylated peptide. It does not bind to a S367D or S367A biotinylated peptide or to an S or WT sequence biotinylated peptide. (*E*) Biolayer interferometry between a PS1-pSer367 biotinylated peptide and an Annexin A2 (AnxA2) or AnxA2-p11 fusion protein at several Ca^{2+} concentrations. The *y* axis represents binding (nanometers). (*F*, *Upper*) Diagram showing the constructs used in this experiment. (*F*, *Lower*) Deletion mutant of Annexin A2 lacking the N terminus (ΔN) does not bind a pPS1 peptide, whereas a deletion mutant of Annexin A2 lacking the third and fourth calcium-binding domains (Δ3–4) is still able to bind a pPS1 peptide. (*G*) In situ PLA between Annexin A2 and PS1 in MEFs derived from WT or PS1-S367A mice. Note the loss of Annexin A2-PS1 binding in the absence of PS1 phosphorylation at Ser367. (Scale bars, 2 μm.)

necessary for its interaction with pPS1 (Fig. 2*F*). To confirm the Annexin A2 and PS1 interaction further, we used an in situ proximity ligation assay (PLA) in cultured cells and demonstrated a close physical relationship between the two proteins (Fig. 2*G*, note red fluorescence in WT cells). The interaction between PS1 and Annexin A2 was abolished in PS1-S367A mutant cells (Fig. 2*G*).

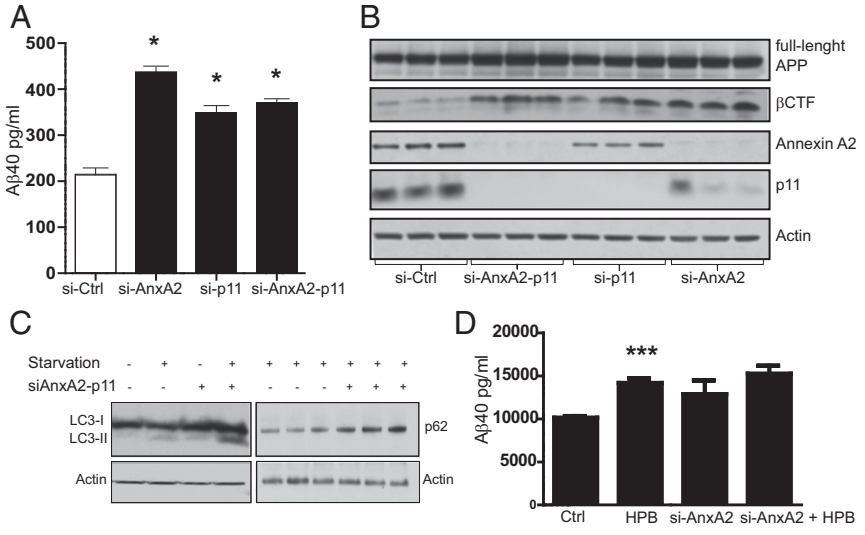

Fig. 3. Annexin A2 regulates Aβ metabolism. (*A*) Knock-down of Annexin A2 and/or p11 increases levels of Aβ40 in N2A cells overexpressing APP. Ctrl, control. (*B*) Knock-down of Annexin A2 and/or p11 increases βCTF levels in N2A cells. (*C*) Knock-down of Annexin A2 and p11 increases LC3-II and p62 protein levels in N2A cells. (*D*) CK1γ inhibitor compound 2-((4-(2-hydroxypropan-2-yl)phenyl)amino)-1*H*-benzo[*d*]imidazole-6-carbonitrile (HPB) increases Aβ levels in cells transfected with a control siRNA, but it fails to increase Aβ levels in cells transfected with siRNA against Annexin A2. Data represent mean ± SEM. $*P < 0.05$, $***P < 0.001$; *t* test. Ctrl, control.

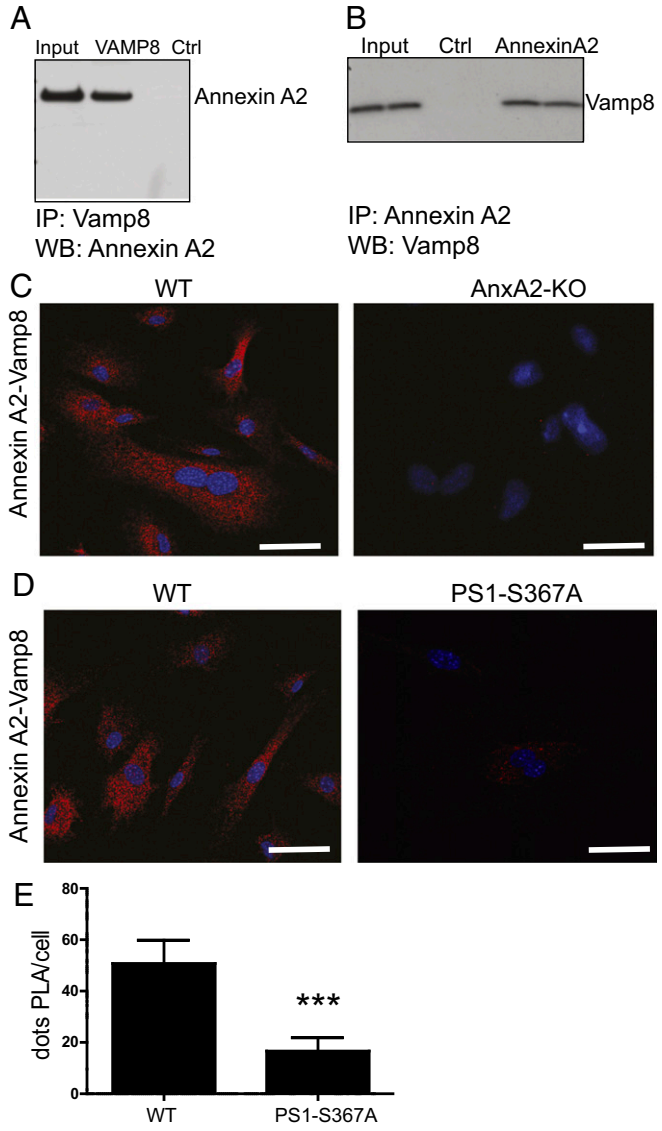

Fig. 4. PS1 phosphorylated at Ser367 modulates binding of Annexin A2 to Vamp8. (*A*) Antibody against recombinant Vamp8 pulls down recombinant Annexin A2 in vitro. (*B*) Immunoprecipitates from whole-mouse brain lysate using anti-Annexin A2 antibody were immunoblotted with an antibody against Vamp8. (*C*, *Left*) Annexin A2 binds Vamp8 in cells, as measured by PLA. (*C*, *Right*) PLA control with fibroblasts derived from AnxA2-KO mice. (Scale bars, 5 μm.) (*D*) In situ PLA between Annexin A2 and Vamp8 in MEFs derived from WT (*Left*) or PS1-S367A mice (*Right*). Note the decrease of Annexin A2-Vamp8 binding in the absence of PS1 phosphorylation at Ser367. (Scale bars, 5 μm.) (*E*) Quantification of PLA from *D* ($n = 15$). Data represent mean ± SEM. ***$P < 0.001$, *t* test. Ctrl, control; WB, Western blot.

Annexin A2 Regulates Aβ Metabolism. We next studied the role of Annexin A2/p11 on Aβ metabolism. N2A cells stably expressing APP695 were transfected with siRNA directed against Annexin A2, p11, or both. Scrambled siRNA was used as a control. Knock-down efficiency was 70–90%, as assessed by immunoblotting. The knock-down of both Annexin A2 and p11 induced a 190% increase in Aβ40 and Aβ42 (Fig. 3*A*). Annexin A2 knock-down also affected the levels of other APP metabolites. The levels of βCTF increased but the levels of total APP did not. The pattern of these changes was the same as shown in the brains of mice with the PS1-Ser367A knock-in (Fig. 3*B*).

Recent reports suggest that Annexin A2 is involved in the early steps of autophagy in primary dendritic cells of the immune system (27). In our experiments, the knock-down of Annexin A2 in N2A cells induced an increase in LC3 II and p62 protein levels, suggesting that the loss of Annexin A2 in these cells resulted in impaired late-stage autophagic flux (Fig. 3*C*). We have shown that CK1γ2 phosphorylates PS1 at Ser367 (22). Knock-down of Annexin A2 blocked the increase in Aβ40 induced by the compound 2-((4-(2-hydroxypropan-2-yl)phenyl)amino)-1*H*-benzo[*d*]imidazole-6-carbonitrile, a CK1γ inhibitor (Fig. 3*D*), confirming the concept that Annexin A2 is functionally linked to the CK1γ2-PS1 phosphorylation pathway.

Annexin A2 Binds Vamp8. Annexin A2 has been shown to bind members of the SNARE protein family, such as SNAP23 (28). We therefore screened SNARE family members for their ability to bind Annexin A2 and found that VAMP8, a lysosomal SNARE, directly binds to Annexin A2 in vitro (Fig. 4*A*). In addition, endogenously expressed Annexin A2 and VAMP8 coimmunoprecipitated from mouse brain lysates, confirming that Annexin A2 and Vamp8 interact in the brain in vivo (Fig. 4*B*). Binding of Annexin A2 to VAMP8 was also confirmed in cells by PLA (Fig. 4*C*, *Left*). As a control for the specificity of the antibodies used for the PLA reaction, PLA between Annexin A2 and Vamp8 was not observed in Annexin A2-KO (AnxA2-KO) cells (Fig. 4*C*, *Right*).

We next analyzed the role of PS1 phosphorylation on Ser367 in Annexin A2/VAMP8 binding. Using PLA in mouse embryonic fibroblasts (MEFs) derived from WT or PS1-367A mice, we found decreased binding of Annexin A2 to VAMP8 in PS1-Ser367A cells, which suggests that pSer-PS1 facilitates Annexin A2–VAMP8 interaction (Fig. 4 *D* and *E*). It has been shown that VAMP8 participates in autophagosome–lysosome fusion by binding to Stx17. Recent reports showed that Stx17, a member of the Qa-SNARE family, translocates to the outer membrane of autophagosomes upon starvation. Here, it recruits the lysosomal R-SNARE, VAMP8, causing fusion of autophagosomes with lysosomes (12). We confirmed the colocalization of STX17 with autophagosomal marker LC3-II upon induction of autophagy by immunofluorescence (Fig. 5*A*). Endogenously expressed Stx17 and Vamp8 coimmunoprecipitated from mouse brain lysates, confirming that Stx17 and Vamp8 interact in the brain in vivo (Fig. 5*B*). This interaction was decreased in the brain of the mutant PS1-Ser367Ala (Fig. 5*B*). The interaction between VAMP8 and Stx17 measured by PLA provided a tool for analyzing the efficiency of autophagosome–lysosome fusion. As a control, we evaluated the effect of autophagy induction on Vamp8-Stx17 binding. We observed an increase in VAMP8-Stx17 binding after inducing autophagy (Fig. 5 *C*, *Upper* vs. *Lower* and *D*). We next analyzed the role of Annexin A2 and pPS1-Ser367 on VAMP8-Stx17 binding using MEFs derived from WT, AnxA2-KO, or PS1-Ser367A mice. We found that loss of Annexin A2 or pPS1-Ser367 significantly decreased the VAMP8-Stx17 binding in cells in situ (Fig. 5 *C*, *Lower* and *D*). Our results suggest that PS1 phosphorylation at Ser367, through interaction with Annexin A2, modulates the progression of autophagy and decreases Aβ levels by facilitating autophagosome–lysosome fusion (Fig. 6).

Discussion

PS1 is an intramembrane protease, harboring the catalytic site of the γ-secretase complex. Although PS1 has a central role in the generation of β-amyloid, little is known about its other possible functions. Here, we describe a phosphorylation site on PS1 that regulates autophagy and promotes the degradation of βCTF.

It was recently found that βCTF can both be a substrate for autophagic degradation and induce impairment of the autophagic/lysosomal (29) and endosomal (30) pathways. These results, together with our findings, suggest the presence of a positive feedback mechanism in which a deficit in autophagy leads to increased βCTF levels, which can, in turn, induce further autophagic impairment.

As a step toward defining the mechanism by which phosphorylated PS1 decreases Aβ levels, we searched for its binding partners and found that Annexin A2 was able to bind specifically to PS1 phosphorylated at Ser367. The S367D analog of PS1 did

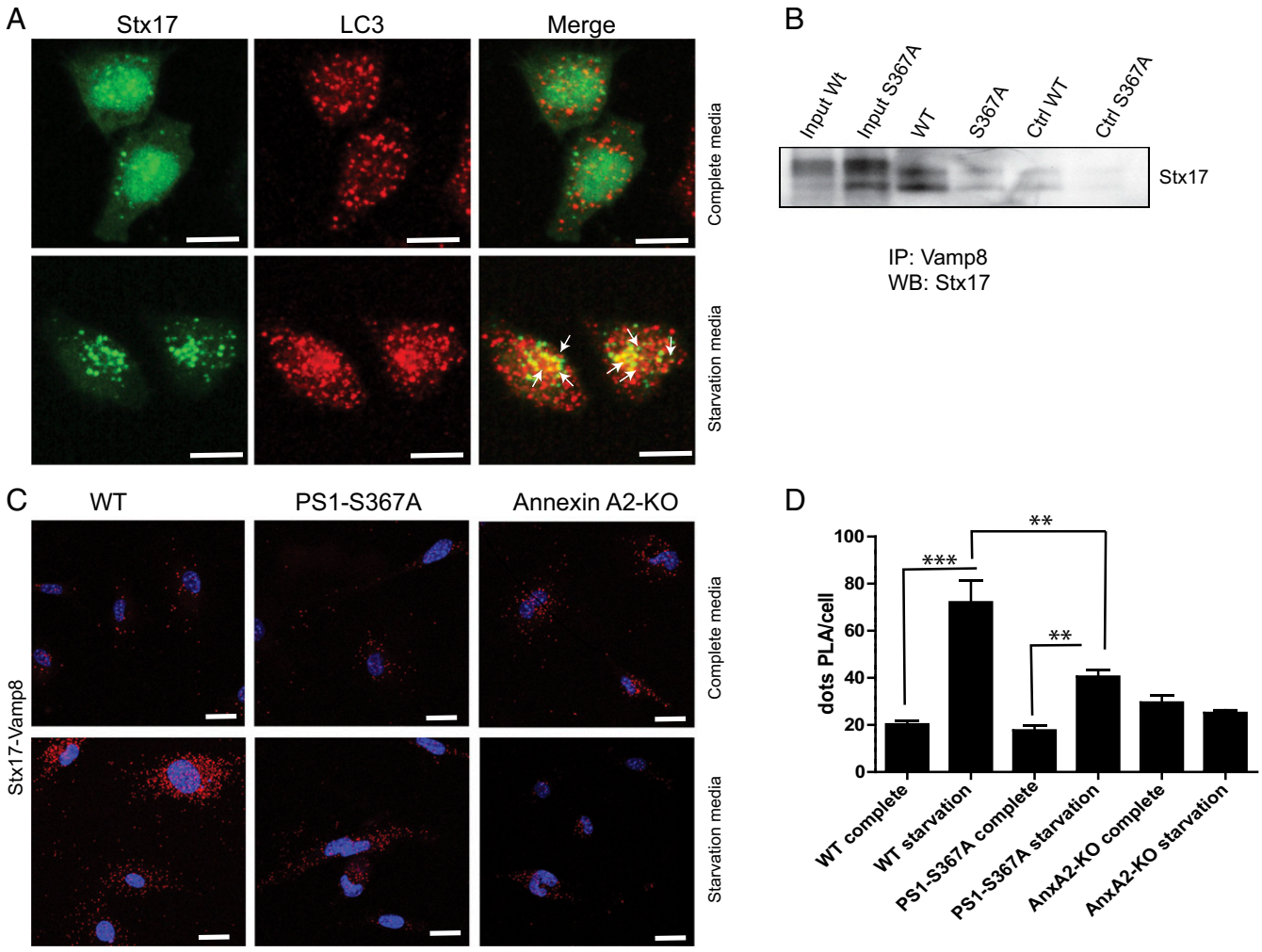

Fig. 5. Annexin A2 facilitates binding of Vamp8 to Stx17. (*A*) Confocal images showing colocalization of Stx17 (green) with $LC3^+$ (red) vesicles when autophagy is induced by starvation. Arrows indicate the site of colocalization. (Scale bar, 5 μm.) (*B*) Immunoprecipitates from whole-mouse brain lysate using anti-Vamp8 antibody were immunoblotted with an antibody against Stx17. Ctrl, control; IP, immunoprecipitation; WB, Western blot. (*C*) In situ PLA between Stx17 and Vamp8 in MEFs derived from WT, AnxA2-KO, or PS1-S367A mice in complete media (*Upper*) or starvation media (*Lower*). (Scale bar, 5 μm.) (*D*) Quantification of number of PLA reactions from *C*. Note the decrease of Stx17-Vamp8 binding in the absence of either Annexin A2 or PS1 phosphorylated at Ser367 ($n = 20$). Data represent mean ± SEM. $^{**}P < 0.01$, $^{***}P < 0.001$; *t* test.

not bind to Annexin A2, providing a molecular explanation for the lack of a phosphomimetic effect of PS1-S367D on Aβ accumulation (22).

A role for Annexin A2 in the early steps of autophagy has recently been described. In primary dendritic cells of the immune system, Annexin A2 promotes ATG16 vesicle biogenesis by orchestrating recruitment of phosphoinositides to vesicular membranes and by coordinating vesicular budding and homotypic fusion (27). In addition, it has been shown that Annexin A2 regulates autophagosome formation in HeLa cells by controlling the sorting and trafficking of ATG9 from endosomes (31). We propose that in addition to autophagosome biogenesis, Annexin A2 plays a role in autophagosome–lysosome fusion. The participation of the same proteins in early and late steps of autophagy may provide greater control of autophagic flux.

We found that Annexin A2 modulates autophagosome–lysosome fusion by interaction with VAMP8, a lysosomal R-SNARE. Vamp8 participates in autophagosome–lysosome fusion by binding Stx17, located in autophagosomes (12). It is possible that Annexin A2 enhances the specificity of the autophagosome–lysosome fusion by targeting a selected pool of lysosomes for fusion with autophagosomes. That these interactions affect a late step in autophagy is supported by the appearance of the vacuoles we observed accumulated in the brain, which are most consistent with autophagosomes that are docked with lysosomes, but not completely fused. However, other effects of this pathway on autolysosome function cannot be excluded.

In the PS1-S367A mouse line, the lack of PS1 phosphorylation at Ser367 prevents its binding to Annexin A2. In turn, Annexin A2 has decreased binding to Vamp8 in the lysosome, rendering the lysosome less able to fuse with the autophagosome. Thus, βCTF present in the autophagosome fails to be degraded in the lysosome. Because γ-secretase has been shown to be active in the autophagosome (32), the increased concentration of βCTF leads to increased synthesis of Aβ. Additional effects of PS1 Ser367 phosphorylation on the autophagic degradation of Aβ and Aβ accumulation are possible.

This study describes a function of PS1 in regulating autophagy. The dephosphorylated PS1 Ser367 form catalyzes the formation of Aβ but does not stimulate the autophagic flux. In contrast, the CK1γ Ser367-phosphorylated form retains its catalytic activity in the formation of Aβ but also causes, as its dominant effect, an enhanced autophagosome–lysosome fusion and the autophagic

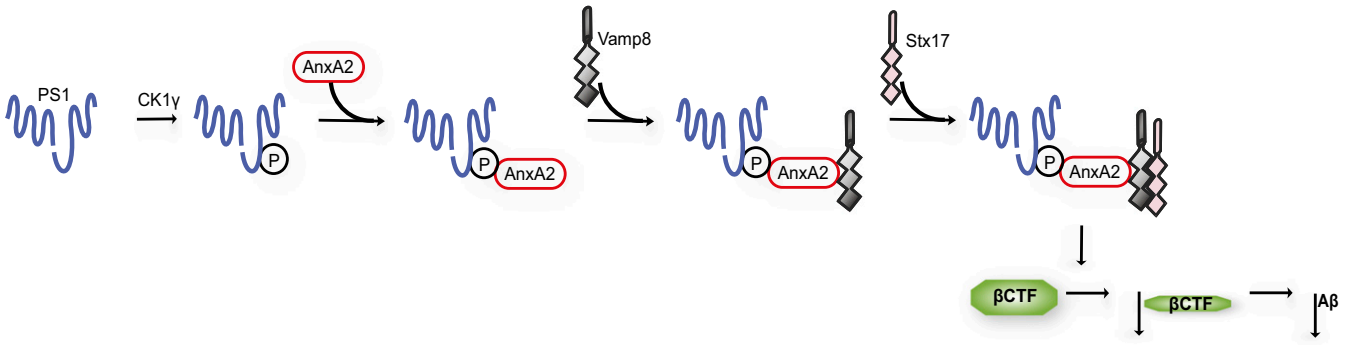

Fig. 6. Proposed model by which PS1 increases autophagic flux and decreases Aβ levels. PS1, upon phosphorylation on Ser367 by CK1γ, interacts with Annexin A2 (AnxA2). In turn, Annexin A2 interacts with Vamp8, which facilitates the binding of Vamp8 to Stx17. This interaction induces the lysosome-autophagosome fusion, triggering the degradation of βCTF, leading to a decrease in Aβ levels. P, phosphorylation.

degradation of βCTF, resulting in a reduced availability of substrate to generate Aβ. Drugs that increase PS1 phosphorylation at Ser367 should aid in the development of potential therapies for Alzheimer's disease.

Methods

All procedures involving animals were approved by the Rockefeller University Institutional Animal Care and Use Committee and were in accordance with the NIH guidelines.

Protein Quantification and Immunoblot Analysis. Detailed descriptions of all experimental procedures used for protein quantification and immunoblot analysis are provided in *SI Methods*.

PLA. Detailed descriptions of all experimental procedures used for PLA are provided in *SI Methods*.

Electron Microscopy. Detailed descriptions of all experimental procedures used for electron microscopy are provided in *SI Methods*.

Statistical Analysis. A detailed description of statistical analysis is provided in *SI Methods*.

ACKNOWLEDGMENTS. We thank Dr. Yotam Sagi and Dr. Jean-Pierre Roussarie for constructive discussion and Elisabeth Griggs for technical assistance. We thank the transgenic services resource center for mouse in vitro fertilization, K. Uryu and the Electron Microscope facility for excellent service, H. Molina for peptide synthesis, and the proteomics center at the W. M. Keck Foundation Biotechnology Resource Laboratory at Yale University. This work was supported by the Fisher Center for Alzheimer's Research Foundation, NIH Grant AG047781, Department of Defense/US Army Medical Research Acquisition Activity (DOD/USAMRAA) Grant W81XWH-09-1-0402, and JPB Grant 475 (to P.G.). V.B. was supported by DOD/USAMRAA Grant W81XWH-14-1-0045. F.S.G. was supported by the NIH/National Institute of Diabetes and Digestive and Kidney Diseases Grant DK098109 and a Veterans Affairs Merit Award.

1. Ohsumi Y (2014) Historical landmarks of autophagy research. *Cell Res* 24:9–23.
2. Suzuki K, Ohsumi Y (2007) Molecular machinery of autophagosome formation in yeast, Saccharomyces cerevisiae. *FEBS Lett* 581:2156–2161.
3. Klionsky DJ, Emr SD (2000) Autophagy as a regulated pathway of cellular degradation. *Science* 290:1717–1721.
4. Nakamura N, Yamamoto A, Wada Y, Futai M (2000) Syntaxin 7 mediates endocytic trafficking to late endosomes. *J Biol Chem* 275:6523–6529.
5. Antonin W, et al. (2000) A SNARE complex mediating fusion of late endosomes defines conserved properties of SNARE structure and function. *EMBO J* 19:6453–6464.
6. Pryor PR, et al. (2004) Combinatorial SNARE complexes with VAMP7 or VAMP8 define different late endocytic fusion events. *EMBO Rep* 5:590–595.
7. Luzio JP, Pryor PR, Bright NA (2007) Lysosomes: Fusion and function. *Nat Rev Mol Cell Biol* 8:622–632.
8. Ward DM, Pevsner J, Scullion MA, Vaughn M, Kaplan J (2000) Syntaxin 7 and VAMP-7 are soluble N-ethylmaleimide-sensitive factor attachment protein receptors required for late endosome-lysosome and homotypic lysosome fusion in alveolar macrophages. *Mol Biol Cell* 11:2327–2333.
9. Fader CM, Sánchez DG, Mestre MB, Colombo MI (2009) TI-VAMP/VAMP7 and VAMP3/cellubrevin: Two v-SNARE proteins involved in specific steps of the autophagy/multivesicular body pathways. *Biochim Biophys Acta* 1793:1901–1916.
10. Furuta N, Fujita N, Noda T, Yoshimori T, Amano A (2010) Combinational soluble N-ethylmaleimide-sensitive factor attachment protein receptor proteins VAMP8 and Vti1b mediate fusion of antimicrobial and canonical autophagosomes with lysosomes. *Mol Biol Cell* 21:1001–1010.
11. Moreau K, Renna M, Rubinsztein DC (2013) Connections between SNAREs and autophagy. *Trends Biochem Sci* 38:57–63.
12. Itakura E, Kishi-Itakura C, Mizushima N (2012) The hairpin-type tail-anchored SNARE syntaxin 17 targets to autophagosomes for fusion with endosomes/lysosomes. *Cell* 151:1256–1269.
13. Guo B, et al. (2014) O-GlcNAc-modification of SNAP-29 regulates autophagosome maturation. *Nat Cell Biol* 16:1215–1226.
14. Diao J, et al. (2015) ATG14 promotes membrane tethering and fusion of autophagosomes to endolysosomes. *Nature* 520:563–566.
15. Liu R, Zhi X, Zhong Q (2015) ATG14 controls SNARE-mediated autophagosome fusion with a lysosome. *Autophagy* 11:847–849.
16. Li Y-M, et al. (2000) Photoactivated γ-secretase inhibitors directed to the active site covalently label presenilin 1. *Nature* 405:689–694.
17. De Strooper B, et al. (1998) Deficiency of presenilin-1 inhibits the normal cleavage of amyloid precursor protein. *Nature* 391:387–390.
18. Thinakaran G, et al. (1996) Endoproteolysis of presenilin 1 and accumulation of processed derivatives in vivo. *Neuron* 17:181–190.
19. LaFerla FM (2002) Calcium dyshomeostasis and intracellular signalling in Alzheimer's disease. *Nat Rev Neurosci* 3:862–872.
20. Begley JG, Duan W, Chan S, Duff K, Mattson MP (1999) Altered calcium homeostasis and mitochondrial dysfunction in cortical synaptic compartments of presenilin-1 mutant mice. *J Neurochem* 72:1030–1039.
21. Pratt KG, Zimmerman EC, Cook DG, Sullivan JM (2011) Presenilin 1 regulates homeostatic synaptic scaling through Akt signaling. *Nat Neurosci* 14:1112–1114.
22. Bustos V, et al. (2017) Bidirectional regulation of Aβ levels by Presenilin 1. *Proc Natl Acad Sci USA* 114:7142–7147.
23. Bai XC, et al. (2015) An atomic structure of human γ-secretase. *Nature* 525:212–217.
24. Gerke V, Creutz CE, Moss SE (2005) Annexins: Linking Ca2+ signalling to membrane dynamics. *Nat Rev Mol Cell Biol* 6:449–461.
25. Morel E, Gruenberg J (2007) The p11/S100A10 light chain of annexin A2 is dispensable for annexin A2 association to endosomes and functions in endosomal transport. *PLoS One* 2:e1118.
26. Liu Y, Myrvang HK, Dekker LV (2015) Annexin A2 complexes with S100 proteins: Structure, function and pharmacological manipulation. *Br J Pharmacol* 172:1664–1676.
27. Morozova K, et al. (2015) Annexin A2 promotes phagophore assembly by enhancing Atg16L$^+$ vesicle biogenesis and homotypic fusion. *Nat Commun* 6:5856.
28. Wang P, Chintagari NR, Gou D, Su L, Liu L (2007) Physical and functional interactions of SNAP-23 with annexin A2. *Am J Respir Cell Mol Biol* 37:467–476.
29. Lauritzen I, et al. (2016) Intraneuronal aggregation of the β-CTF fragment of APP (C99) induces Aβ-independent lysosomal-autophagic pathology. *Acta Neuropathol* 132:257–276.
30. Jiang Y, et al. (2016) Partial BACE1 reduction in a Down syndrome mouse model blocks Alzheimer-related endosomal anomalies and cholinergic neurodegeneration: Role of APP-CTF. *Neurobiol Aging* 39:90–98.
31. Moreau K, et al. (2015) Transcriptional regulation of Annexin A2 promotes starvation-induced autophagy. *Nat Commun* 6:8045.
32. Yu WH, et al. (2004) Autophagic vacuoles are enriched in amyloid precursor protein-secretase activities: Implications for β-amyloid peptide over-production and localization in Alzheimer's disease. *Int J Biochem Cell Biol* 36:2531–2540.